Improving Signal/Noise Resolution in Single-Molecule Experiments Using Molecular Constructs with Short Handles

N. Forns,[†] S. de Lorenzo,[¶] M. Manosas,[‡ †] K. Hayashi,[§] J. M. Huguet,[†] and F. Ritort[†¶]

[†]Departament de Física Fonamental, Facultat de Física, Universitat de Barcelona, Barcelona, Spain; [‡]Laboratoire de Physique Statistique, École Normale Supérieure, Unité Mixte de Recherche 8550 associée au Centre National de la Recherche Scientifique et aux Universités Paris VI et VII, Paris, France; [§]Institute of Scientific and Industrial Research, Osaka University, Mihogaoka, Ibaraki, Osaka, Japan; and [¶]CIBER de Bioingeniería, Biomateriales y Nanomedicina, Instituto de Sanidad Carlos III, Madrid, Spain.

SUPPORTING MATERIAL

S1. Free energy landscape and design of DNA hairpins

The mechanical folding and unfolding of nucleic acid hairpins is commonly described in terms of a reaction coordinate and the corresponding free energy landscape (1-4) (see Fig. S1). When subject to force, the end-to-end distance of the molecule along the force axis is an adequate reaction coordinate for the folding-unfolding reaction pathway. For a given applied force f it is common to consider only a single kinetic pathway for the unfolding and folding reactions, which is characterized by a single transition state (TS). The TS is the highest free energy state along the reaction coordinate and determines the kinetics of the folding-unfolding reaction. This model involves four parameters: the free energy difference between states S and S', $\Delta G_{SS'} = G_{S'} - G_S$; the height of the kinetic barrier B, defined as the free energy difference at force f between the TS and the S state; and the distances $x^{\ddagger}_{SS'}$ and $x^{\ddagger}_{S'S}$ along the reaction coordinate that separates the TS from the S and S' states respectively. The total distance between S and S' is defined as $x_{SS'}$ ($x_{SS'} = x^{\ddagger}_{SS'} + x^{\ddagger}_{S'S}$). The distances and free energy differences between the different states (S, S' and TS) determine the force kinetics of unfolding/folding. Under an applied force the free energy landscape is tilted along the reaction coordinate changing the free energy difference $\Delta G_{SS'}$ and the barrier B. In a first approximation $\Delta G_{SS'}$ and B change linearly with the force whereas $x^{\ddagger}_{SS'}$ and $x^{\ddagger}_{S'S}$, are taken as constant. This simplified representation can be generalized to include intermediates on-pathway.

In order to design the hairpins we have calculated the force-dependent molecular free energy landscapes by including the entropic contribution due to the stretching of the released ssDNA into the free energy landscape as predicted by the nearest-neighbor model (5). For the elastic response of the ssDNA we use the inextensible worm-like chain model (WLC) defined by,

$$F_{WLC}(x) = (k_B T/p)\left[\left(1/4(1-x/L_0)^2\right) - (1/4) + (x/L_0)\right], \qquad \text{(S1)}$$

where k_B is the Boltzmann constant and T is the temperature, p stands for the persistence length and L_0 is the contour length, $L_0 = n \times a$ where a=0.59 nm and n is the total number of bases of the unfolded hairpin. For the persistence length we used values in the range 1.0-1.5nm that fit the experimentally measured force/distance jump at coexistence (see Section S5). Other models for the elastic behavior such as the freely jointed chain give very similar results.

To calculate the free energy landscapes shown in Fig. 2 *B* and Fig. 3 *B* we use the following formula,

$$G(n,f) = G_0(n) + G_{ssDNA}(0 \rightarrow x_n; f) - fx_n = G_0(n) - \int_0^f x_{FJC}(f')df', \qquad \text{(S2)}$$

where we used $G_{ssDNA}(0 \rightarrow x_n; f) = \int_0^{x_n} F_{WLC}(x)dx$ with $f = F_{WLC}(x_n)$ as given in Eq. S1. Here x_n stands for the molecular extension of *2n* bases of ssDNA (corresponding to the release of *n* bp of dsDNA) stretched at force *f*. The values for $G_0(n)$ can be obtained from Mfold (5,6) by adding the nearest-neighbor base pair free energies along the hairpin sequence. For $n=N$ (where *N* stands for the total number of base pairs in the hairpin) the total number of bases is equal to *2n* plus the number of bases in the loop. Moreover, $G(n=N,f)$ must be corrected by adding the term $G_d(f)$ to account for the finite diameter d_0 of the hairpin which, in the presence of a force *f*, tends to be oriented along the force axis. The free energy cost to orient a dipole of length d_0 along an applied force *f* is given by,

$$G_d(f) = k_B T \ln[\sinh(\beta f d_0)/(\beta f d_0)], \qquad \text{(S3)}$$

and the corresponding extension of the dipole is equal to

$$d(f) = d_0 \coth(\beta f d_0) - (1/\beta f), \qquad \text{(S4)}$$

Note that in the limit $\beta f d_0 >> 1$ the value of $d(f)$ approaches d_0 whereas $G_d(f)$ is approximately equal to $f d_0$, the value typically employed in the literature to estimate the diameter contribution (9). For our calculations we took d_0=2 nm. This was the procedure we used for the 2S hairpin.

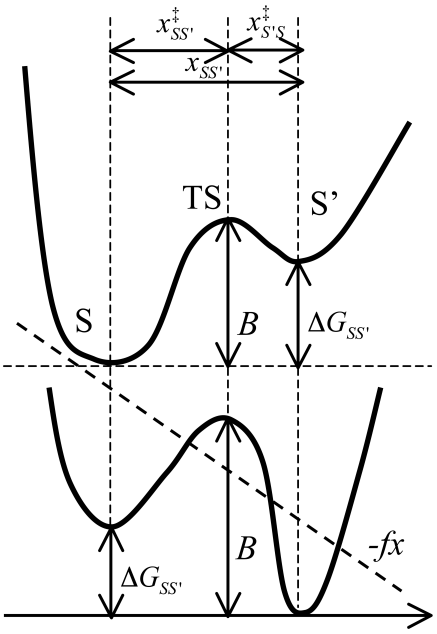

FIGURE S1 Schematic picture of the two-state model. The free energy landscape of the molecule along the reaction coordinate axis *x* at a given force has two minima corresponding to the two states *S* and *S'*. When a mechanical force is applied to the ends of the molecule the free energy landscape is tilted along *x*, decreasing de free energy of the *S'* state and the *TS* relative to the *S* state.

S2. Synthesis of DNA hairpins with short and long handles and molecular setup

The DNA hairpins (Section S1) with short handles are synthesized using the hybridization of three different oligonucleotides (Fig. 1 *B,* main text). One oligonucleotide contains the sequence of the ssDNA left handle plus a part of the sequence of the desired DNA hairpin; the second has the rest of the sequence of the DNA hairpin and the ssDNA right handle. The right and the left ssDNA handles have the same sequence to hybridize them with the third oligonucleotide. The first oligonucleotide has a biotin at its 5' end and the second oligonucleotide has been modified at its 3' end with a digoxigenin tail (DIG Oligonucleotide Tailing Kit, 2nd generation, Roche Applied Science, Barcelona, Spain). Once the first and the second oligonucleotides are hybridized to form the hairpin, the third oligonucleotide is hybridized to the handles to form the dsDNA handles of 29 bp each. All the oligonucleotide sequences used in this construction are shown in Fig. S2.

The 2S and 3S hairpins with long handles consist of a single DNA hairpin attached at its 5' and 3' end to long dsDNA handles used for pulling (Fig. S2 *A*). The left handle was synthesized through a PCR reaction using the pBR322 plasmid as a sample and the primers left-Biotin and left-Tsp45I (Fig. S2 *B*). The primer left-Biotin has a biotin at its 5' end. The product of the PCR was digested with the *Tsp*45I restriction enzyme (New England Biolabs, UK), giving a 528 bp dsDNA fragment with a biotin at one end and a nonpalindromic *Tsp*45I overhang at the other end. The right handle was obtained after two consecutive digestions of λ DNA. First, λ DNA is digested with *Sph*I enzyme (New England Biolabs, UK) and the 2216 bp fragment was gel purified. This fragment was digested again with *Tsp*RI (New England Biolabs, UK) and the 874 bp DNA gel purified. This dsDNA has at one end the cosL overhang of λ and at the other end a nonpalindromic *Tsp*RI sticky end. The cosL overhang was hybridized with the soc-Le oligonucleotide (Fig. S2 *B*) that was previously modified at 3' end with a digoxigenin tail (DIG Oligonucleotide Tailing Kit, 2nd generation, Roche Applied Science, Spain). The 2S and 3S DNA hairpins constructs are based on an oligonucleotide that has the desired sequence flanked by the two sticky ends (*Tsp*45I and *Tsp*RI) (Fig. S2 *B*). Finally, the hairpin was annealed and ligated to the two dsDNA handles to obtain the molecular construction.

Streptavidin-coated polystyrene microspheres (1.87 μm; Spherotech, Libertyville, IL) and protein G microspheres (3.0-3.4 μm; G. Kisker Gbr, Products for Biotechnologie, Steinfurt, Germany) coated with anti-digoxigenin polyclonal antibodies (Roche Applied Science, Spain) were used for specific attachments to the DNA molecular constructions described above. Attachment to the anti-digoxigenin microspheres was achieved first by incubating the beads with the tether DNA. The second attachment was achieved in the fluidics chamber and was accomplished by bringing a trapped anti-digoxigenin and streptavidin microspheres close to each other.

A

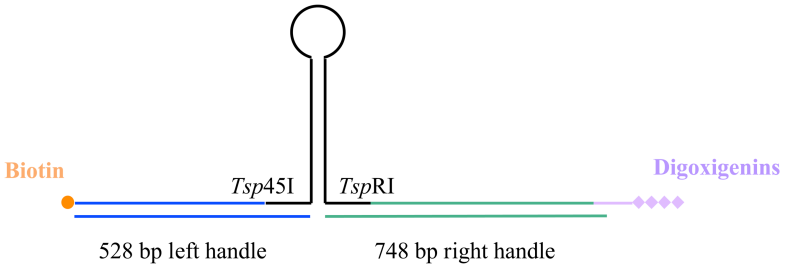

B

Primers PCR left handle
TTC TTG AAG ACG AAA GGG CCT
CCATTGCTGCAGGCATCGTG
soc-Le oligonucleotide
AGGTCGCCGCCCAAAAAAAAAAAA
2S hairpin
GTCACGCGAGCCATAATCTCATCTGGAAACAGATG AGATTATGGCTCGC**GGCAGTGTT**
3S hairpin
GTCACGCGTCGCAGCGCCAAAAGGCAGGCGGAAA GAGCGCCTGCCTTTTCGCTGCGACGC**GGCAGTGTT**

C

2S hairpin	
1st oligo	**AGTTAGTGGTGGAAACACAGTGCCAG CGC**GCGAGCCATAAT
2nd oligo	CTCATCTGGAAACAGATGAGATTATGGC TCGC**AGTTAGTGGTGGAAACACAGTG CCAGCGC**
3S hairpin	
1st oligo	**AGTTAGTGGTGGAAACACAGTGCCAG CGC**GCGTCGCAGCGCCAAAAGGCAGGC GGAAAGAGCGCCTGCCTTTTCGCTG
2nd oligo	CGACGC**AGTTAGTGGTGGAAACACAG TGCCAGCGC**
3rd oligo	
GCGCTGGCACTGTGTTTCCACCACTAACT	

FIGURE S2 (*A*) Molecular construct with dsDNA long handles, left handle (528bp) made by PCR reaction and right handle (748 bp) obtained from λ DNA. (*B*) In the table are listed the oligonucleotides used to make the long handles construction. The 2S and 3S hairpins sequences have in bold the two sticky ends (*Tsp*45I and *Tsp*RI). (*C*) Sequences used to synthesize the two hairpins with short handles. In bold is shown the part of the sequence that corresponds to the handle.

S3. Experimental setup, hopping and pulling experiments

The experiments have been carried out using a high stability newly designed miniaturized dual-beam optical tweezers apparatus (3,8). It consists of two counter-propagating laser beams of 845 nm wavelength that form a single optical trap where particles can be trapped by gradient forces. The DNA hairpin is tethered between two beads (Fig. 1 *A*). One bead is immobilized in the tip of a micropipette that is solidary with the fluidics chamber; the optical trap captures the other bead. The light deflected by the bead is collected by two photodetectors located at opposite sides of the chamber that produce a direct measure of the total change in light momentum which is equal to the net force acting on the bead. Piezo actuators coupled to metallic wigglers that bend the optical fibers can move the optical trap.

The folding-unfolding experiments described in this report were performed at ambient temperature (25ºC) in a buffer containing 10 mM Tris-HCl pH7.5, 1 mM EDTA, 1 M NaCl, 0.01% Sodium Azide. Two types of hopping experiments were done for the DNA hairpin constructs:

1. CFM (4,10,11): the force applied to the DNA constructs was maintained to a preset value (usually between 12 and 15 pN) by moving the piezo actuators through a feedback control (4) that operates at 1kHz. We can observe the molecule hopping between different extensions depending on the state of the hairpin (Fig 2F and Fig 3F main text).

2. PM (10,11): in this case the position of the trap is kept constant (without feedback) and allowing the captured bead to passively move in the optical trap. Thus the trapped bead changes position inside the trap in response to the end-to-end distance change of the molecular construct. Consequently, the force hops among different levels corresponding to the different states of the hairpin (Fig 2D and Fig 3D main text). By moving the trap to a new position, the value of the tension on the hairpin in the different (folded, unfolded and intermediate) states changes, modifying the equilibrium (Boltzmann-Gibbs) weights of these states. This kind of experiment allowed us to measure the kinetic rates over different forces.

In pulling experiments the optical trap is moved at a constant speed and the molecule pulled (13,14) until a value of the force is reached such that the molecule unfolds. If the pulling process is reversed then the molecule refolds again. In these experiments the force exerted upon the system is recorded as the function of the trap relative distance giving the so-called force-distance curve (FDC). The folding and refolding of the molecule can be identified as force-distance jumps observed in the FDC. In all cases data were collected at 1 kHz.

S4. Data analysis

Detailed balance condition Eq. 2 can also be applied to the PM case, where the control parameter is the position of the trap relative to the pipette, X_T, rather than the force. In that latter case we can expand the free energy difference between states S and S' in the vicinity of the coexistence distance X_T as: $\Delta G_{SS'}(X_T) = -(X_T - X_T^c)\Delta f$, where Δf is the (positive) force jump between the folded and unfolded branches. This expression tells us that at coexistence (X_T=X_T^c) the two states have the same free energy and, along each branch, we have f=$\partial G/\partial X_T$. By using the relation Δf=$\varepsilon_{eff}\, x_m$ with ε_{eff} and x_m the effective stiffness and the molecular extension of ssDNA released at the transition we get, $\Delta G_{SS'}(\overline{f}) = -(\overline{f} - \overline{f_c})\frac{\Delta f}{\varepsilon_{eff}} = -(\overline{f} - \overline{f_c})x_m = \Delta G_{SS'} - \overline{f}x_m$ where $\overline{f}$ is average force between the folded and the unfolded branches at a given X_T and $\Delta G_{SS'} = \overline{f^c}x_m$ is the free energy of formation at zero force plus the stretching contribution of the extended ssDNA. Therefore Eq. 2 can be also used in the PM case replacing the force f by the average force between the folded and the unfolded branches, $\overline{f}$.

For the PM hopping experiments of the two-states 2S hairpin, folding and unfolding transition rates were calculated from the time-dependent force traces (10) (Fig. 2*D*). Each trace normally contained 50-150 cycles of unfolding/refolding events, which showed no significant force drift. Distributions of the force were fitted to Gaussian functions for the folding and unfolding processes (examples are shown in Fig. 2*E*),

$$P(f) = \left(w \Big/ \left(2\pi\sigma_F^2\right)^{1/2}\right) e^{-\left(\left(f-f^F\right)^2 \Big/ 2\sigma_F^2\right)} + \left(1-w \Big/ \left(2\pi\sigma_U^2\right)^{1/2}\right) e^{-\left(\left(f-f^U\right)^2 \Big/ 2\sigma_U^2\right)}, \qquad \text{(S5)}$$

where *P(f)* is the normalized number of counts for each binned force f; w and *1-w* are the statistical weights of the unfolded and folded states and σ_n^2 (n = U or F) are the widths of the Gaussian peaks, respectively; f^U and f^F are the average forces at the unfolded and folded states, respectively; States (folded or unfolded) of the hairpin along the force trace were assigned according to whether the instantaneous force was closer to f^U or f^F. Transition rates were computed as the inverse of the mean lifetime for each state. From Eq. 1a and Eq. 1b and doing linear fits of the logarithm of the rates versus force, we can extract the free energy difference between states F and U by using the expression,

$\Delta G_{FU} = k_B T\left[\log(k_{U\to F}) - \log(k_{F\to U}) + fx_{FU}\right]$, but using the Eq. 2 we can also obtain these values.

For the 3S hairpin PM hopping (see Fig. 3*D* for an experimental trace) we applied the same data analysis as for the 2S hairpin but including the intermediate state, I. We assume that to go from F to U and vice versa the hairpin always goes through I; therefore, four different transition rates were obtained: transition rates from F to I, from I to F, from I to U and finally from U to I. Distributions of the force were fitted to three Gaussian functions for the F, I and U states (Fig. 3*E*),

$$P(f) = \left(w_U \Big/ \left(2\pi\sigma_U^2\right)^{1/2}\right) e^{-\left(\left(f-f^U\right)^2 / 2\sigma_U^2\right)} + \left(w_F \Big/ \left(2\pi\sigma_F^2\right)^{1/2}\right) e^{-\left(\left(f-f^F\right)^2 / 2\sigma_F^2\right)}$$
$$+\left(1 - w_F - w_U \Big/ \left(2\pi\sigma_I^2\right)^{1/2}\right) e^{-\left(\left(f-f^I\right)^2 / 2\sigma_I^2\right)} \quad \text{(S6)}$$

where $P(f)$ is the normalized number of counts for each binned force f; w_U, w_F and $w_I = 1 - w_F - w_U$ are the statistical weights of the U, F and I states and σ_n^2 (n = U, F or I) are the widths of the Gaussian peaks, respectively; f^U, f^F and f^I are the average forces at the U, F and I states, respectively; States (F, U and I) of the DNA along the force trace were assigned according to whether the instantaneous force was closer to f^U, f^F and f^I. Transition rates were computed as the inverse of the mean lifetime for each state. The free energy difference $\Delta G_{SS'}$ between any pair of states S, S´ (F, U and I) is obtained from the rates Eq. 1a and Eq. 1b and using the Eq. 2 as we did for the hairpin 2S.

For the CFM, transition rates and free energy differences were calculated from the time-dependent extension traces (Fig. 2 *F* and Fig. 3 *F*). Hopping traces usually contain 50-150 folding/refolding cycles. As the measured extension traces may drift over the time period, we applied a different strategy to analyze these data. A transition between the F and U states in the 2S hairpin was considered to occur when the extension changed by at least 60 % of the average total extension difference between both states, and by at least 50 % of the extension difference between the F and I states and between the I and U states for the 3S hairpin.

S5. Folding free energy at zero force

From hopping experiments we have determined the different values of $\Delta G_{SS'}$ for the different hairpins (Table 1). To extract the free energy difference between different states at zero force ($\Delta G^0_{SS'}$) we must subtract to the experimentally determined $\Delta G_{SS'}$ from Eq. 1a, Eq. 1b and Eq. 2 the contribution of mechanical stretching of the ssDNA at the coexistence force (9) as well as the orientation of the hairpin. The most straightforward way of doing this is by measuring the value of the coexistence force and the released molecular extension and to use the WLC model with parameters previously given (see Section S1),

$$\Delta G^0_{SS'} = \int_0^{f^C_{SS'}} x_{WLC}(f')df - k_B T \ln\left[\sinh\left(\beta f^C_{SS'} d_0\right)\Big/\left(\beta f^C_{SS'} d_0\right)\right], \qquad \text{(S7)}$$

where $f^C_{SS'}$ stands for the coexistence force between states S and S' and d_0 is the diameter of the hairpin (taken equal to 2 nm). The second term in the rhs of Eq. S7 corresponds to the free energy correction due to the orientation of the hairpin along the force axis (Section S1 and Eq. S3). Let us stress that previous expression Eq. S7 does not require to include the free energy correction expected from the contraction/expansion of handles or the repositioning of the bead when the molecule hops.

How do we estimate the value of $\Delta G^0_{SS'}$? We proceed as follows. In the CFM handles and bead contraction are not expected because the force is kept constant. Therefore we used the following expression,

$$x_{WLC}(f^0_{SS'}) = \Delta x_{SS'} + d(f^0_{SS'}), \qquad \text{(S8)}$$

where $\Delta x_{SS'}$ is the experimentally measured average molecular extension jump between the states S and S' along the hopping trace at coexistence and $d(f^0_{SS'})$ is the average extension contributed by the orientation of the hairpin as given in Eq. S4. We then determined the persistence length value for the ssDNA such that Eq. S8 holds. Using these values in Eq. S7 we could then determine the value of $\Delta G^0_{SS'}$.

In PM experiments the change in force when the molecule hops induces changes in the molecular extension of the handle and the bead position. In this case it is easy to prove (see Appendix C in (9)) that

$$x_{WLC}(f^C_{SS'}) = \left(\Delta f_{SS'}\big/\varepsilon_{eff}(f^C_{SS'})\right) + d(f^C_{SS'}), \qquad \text{(S9)}$$

where $\Delta f_{SS'}$ is the average force jump between the states S and S' along the hopping trace at

coexistence and $\varepsilon_{eff}(f^C_{SS'})$ is the effective rigidity of the molecular setup (bead and handles) in the high force state (might be S or S') at coexistence. In order to extract the folding free energy at zero force we determined the value of the persistence length for the ssDNA such that released extension agrees with the experimental estimate obtained from Eq. S9. The same procedure was used in the CFM, obtaining identical elastic ssDNA parameters. Using these values in Eq. S7 we could then determine the value of $\Delta G^0_{SS'}$.

In all conditions we investigated (DNA sequence, PM versus CFM hopping, long handles versus short handles) the values obtained for $\Delta G^0_{SS'}$ agree reasonably well with the values estimated from the unified oligonucleotide parameters used by Mfold servers to predict folding free energies (5). However, as it is well known, this is strongly dependent on the model used to describe the ideal elastic properties of the ssDNA.

TABLE S5 Folding free energy at zero force of 2S and 3S hairpins.

	x_{FU}	f^C_{FU}	G_d	G_{ssDNA}	ΔG^0_{FU}	ΔG^0_{MFold}
2S	18.3 ±0.9	14.8 ±0.7	1.7	16.6 ±0.2	50.9 ±0.7	50.7
	x_{FI}	f^C_{FI}	G_d	G^{ssDNA}_{FI}	ΔG^0_{FI}	ΔG^{FI}_{MFold}
3S	12.0 ±0.6	14.5 ± 0.7	-	9.7 ± 0.2	32.6 ±3.5	33.9
	x_{IU}	f^C_{IU}	G_d	G^{ssDNA}_{IU}	ΔG^0_{IU}	ΔG^{IU}_{MFold}
3S	10.0 ±0.7	12.8 ±0.6	1.5	9.9 ±0.1	22.7 ±3.3	27.2

Results of the 2S hairpin in the first row and the results for 3S hairpin in the two last rows. To measure the folding free energies at zero force we used the coexistence forces and extensions given in Table 1. The forces are given in pN, the extensions in nm and the energies in k_BT. Stretching contributions were estimated using the elastic parameters reported in Section S5. For the 2S hairpin we took a total number of bases N equal to 44 and hairpin diameter d=2 nm. For the 3S hairpin we took N=26 and d=0 between states F and I and N=29 and d=2 nm between states I and U. Uncertainties in free energies were estimated by propagating the experimental errors obtained for the values of the molecular extension and the coexistence force. Statistics of molecules indicated in the caption of Table 1.

S6. Rigidity of the optical trap

The measurement of the power spectrum is a calibration method that uses the thermal fluctuations of a bead in the optical trap to determine the stiffness of the trap. The experiments have been carried out with calibration beads of 3 μm of diameter in the same buffer where we did the experiments with hairpins. The force fluctuations have been measured at an acquisition rate of 50 kHz using a data acquisition board (National Instrument PXI-1033), which allows us to achieve a wide range of frequencies. The power spectral density has been calculated from 500000 data points. Fig. S6 shows the power spectrum obtained by the Fourier transform of the experimental data. The power spectrum has been fitted to a theoretical Lorentzian function,

$$\langle \Delta f^2(\nu) \rangle = \left(2\xi k_B T \omega_c^2\right) \Big/ (\omega_c^2 + (2\pi\nu)^2) = S^2 \left(a \Big/ (b + (2\pi\nu)^2)\right), \qquad \text{(S10)}$$

where ν is the frequency in Hz, ω_c is the corner frequency in rad/s ($\omega_c = 2\pi\nu_c$), ξ corresponds to the drag coefficient, S is the conversion factor from Volts to pN, and a and b are the fitting parameters of the Lorentzian function.

By fitting Eq. S10 to the power spectrum and from the knowledge of the value of the drag coefficient we can determine the conversion factor S and ω_c. The value of ξ has been obtained from a measurement of the viscosity (η) of the buffer in a viscosimeter and using the relation $\xi = 6\pi\eta r$ with r=1.5 μm (the radius of the calibration bead). We find $\xi = 2.78\times10^{-5}$ pN s/nm, $S \cong 23$ pN/V S and ω_c=2293 Hz. The stiffness of the optical trap ε_b is obtained with the equation:

$$\varepsilon_b = \omega_c \xi \,, \qquad \text{(S11)}$$

where we obtain a stiffness value of 0.064 pN/nm.

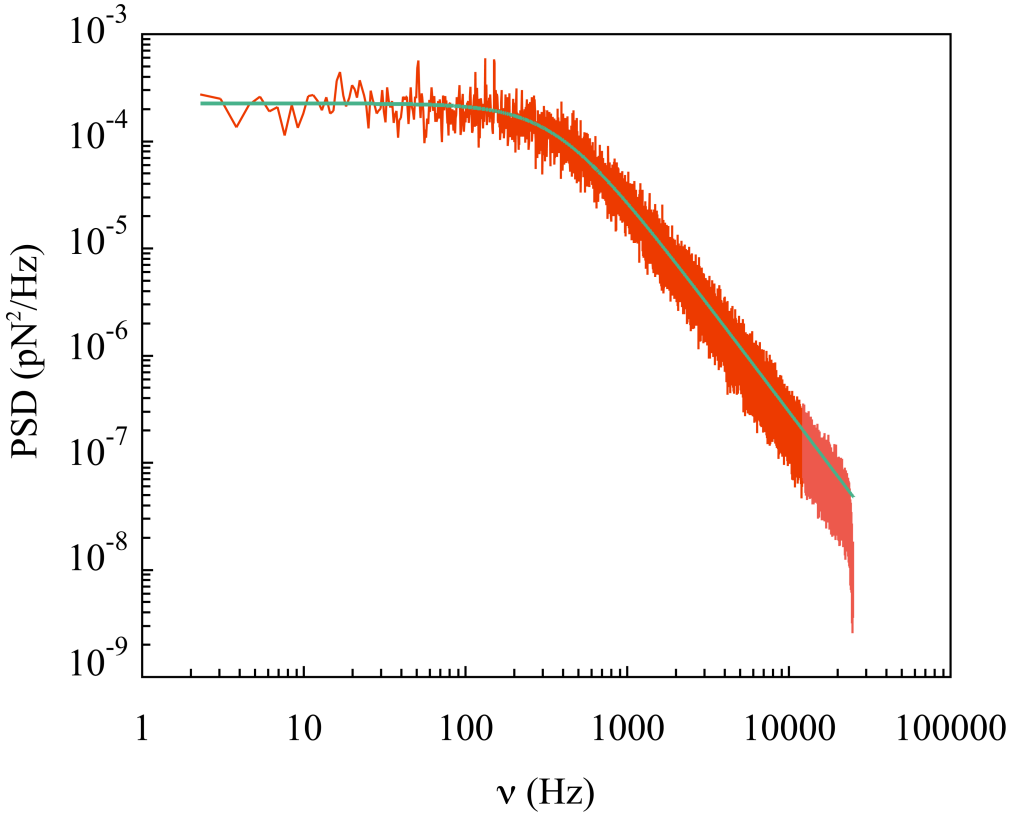

FIGURE S6 Calibration by thermal noise. Power spectrum of the Fourier transform of the fluctuation force data of the bead in the optical trap (in *red*) and the Lorentzian fit (in *green*)

S7. Apparent rates versus passive mode rates at high and low trap stiffness

Under PM conditions the folding/unfolding rates can be plotted or represented in two different ways: as a function of the average force in the folded and unfolded states (this is the standard representation adopted throughout this paper) or as a function of the trap position (the true control parameter in PM experiments). The apparent coexistence rate k_{app}^{C} is the value of the folding/unfolding transition rate in the latter representation, where both states (F and U) are equally populated. Note that k_{app}^{C} differs from the PM coexistence rates, k_{FU}^{C}, also measured in the same PM experiments. Because the PM coexistence rates have been found to be nearly equal to the coexistence rates in the CFM, they seem a more robust indicator about force kinetics than the apparent coexistence rates (10,11). This is the reason why we adopted PM rates throughout this paper. According to (12) (see the Supplementary Material shown in (11) as well), the apparent coexistence rate k_{app}^{C} should decrease when the trap stiffness decreases and should be larger than the CFM or PM coexistence rates k_{FU}^{C} (obtained from the crossing points of the linear fits of the k_{FU} and k_{UF}) (10,11). Similarly one might expect that the apparent coexistence rate k_{app}^{C} should decrease for longer handles as compared to short

handles. Strikingly enough, this is the contrary of what we find for the PM coexistence rates: they tend to increase for longer handles, i.e. when the effective rigidity of the molecular setup decreases. Is there a discrepancy between our results and those reported in (12)? We have challenged this apparent contradiction by doing PM hopping experiments at high (0.064 pN/nm) and at low (0.020 pN/nm) trap stiffness with the 2S hairpin with short and long handles (see Fig. S7 and Table S7). As expected we have found that k_{app}^{C} is always higher than the PM coexistence rate. Our results also confirm the striking dependences reported in this and previous works: although PM coexistence rates increase either by decreasing the power of the trap or increasing the length of the handles, the values of k_{app}^{C} follow the reverse tendency and increase as the effective rigidity of the setup is decreased.

Note that the difference in kinetics between apparent and coexistence rates for short and long handles can be explained in terms of the force jump measured in the passive mode which is proportional to the effective stiffness of the setup formed by the trap serially connected to the handles. Because the stiffness of the handles (short and long) that are pulled at approximately 14pN is much higher than the stiffness of the trap, the effective stiffness is approximately equal to the stiffness of the trap. In Figure S7-2 we show an illustration of such effect. Consequently, the ratio k_{app}^{C} / k_{FU}^{C} is ~ 3.2 for both long and short handles at 0.06 pN/nm, and ~1.5 for both handle lengths at 0.02 pN/nm, i.e. to a very good approximation it is only dependent on the trap stiffness.

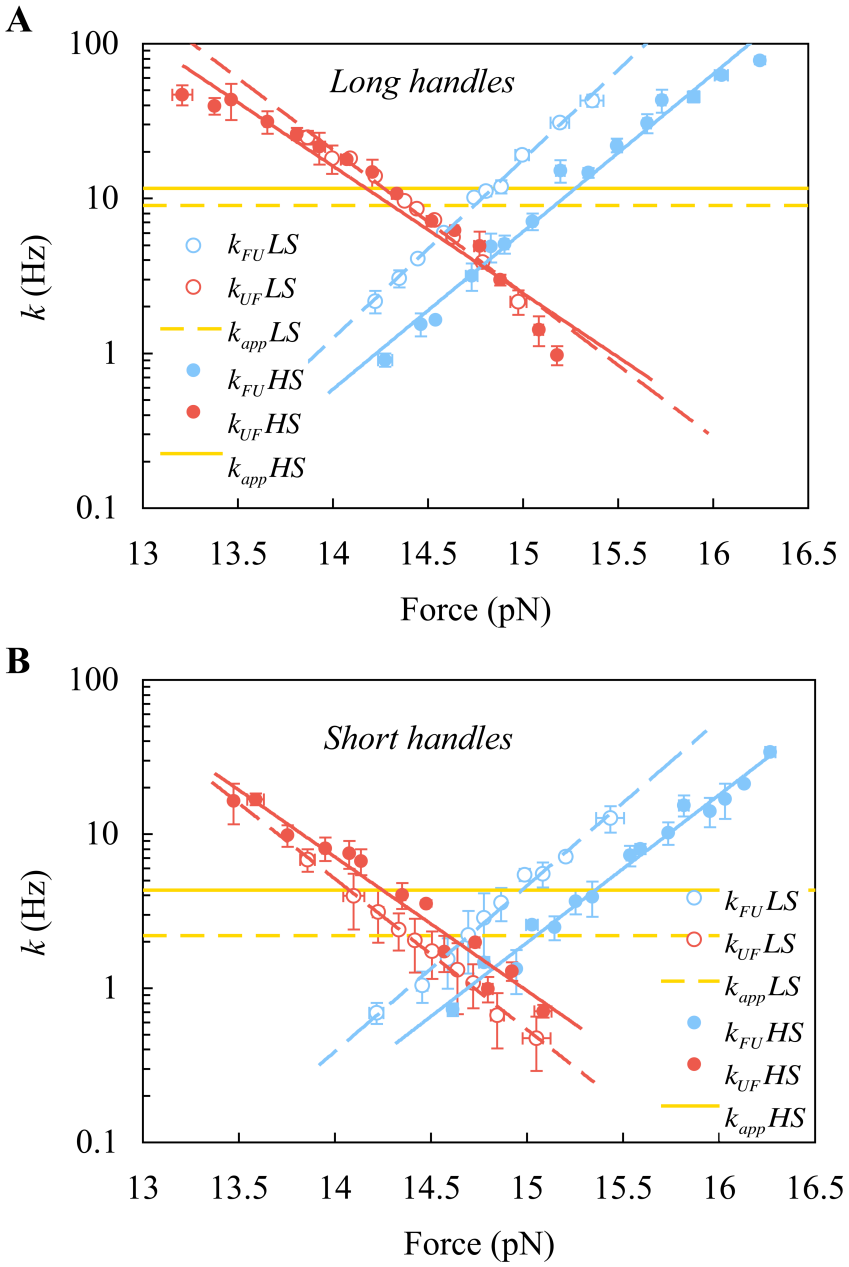

FIGURE S7 Apparent coexistence rates for 2S hairpin with long handles. (*A*) and short handles (*B*). Plots of the *k* as a function of force for PM experiments done at low trap stiffness (*open circles*) and at high trap stiffness (*solid circles*) and their linear fit (*dotted lines* for low trap stiffness and *solid lines* for high trap stiffness). The k_{FU} is shown in *blue* and the k_{UF} is shown in *red*. The apparent coexistence rates are shown for low (*yellow dotted line*) and high trap stiffness (*yellow solid line*). The values are obtained averaging 2 molecules for low trap stiffness and 5 and 7 molecules for high stiffness with short and long handles respectively.

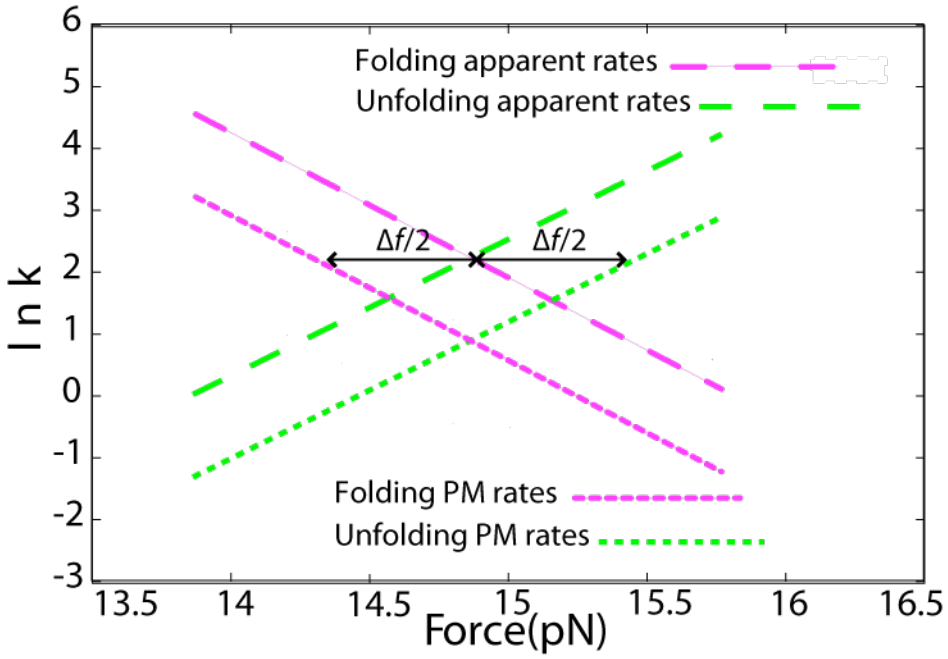

FIGURE S7-2: Schematics of the logarithm of the kinetic rates versus force representation for the apparent rates and PM rates measured in the PM. The switch between the lines correspond to the jump in force Δf between folded and unfolded branches.

TABLE S7 Coexistence rates of 2S hairpin with long and short handles

	Long handles		**Short handles**	
	0.064 pN/nm	**0.020 pN/nm**	**0.064 pN/nm**	**0.020 pN/nm**
k_{app}^{C}	11.7 ±0.6	9.07 ±0.06	4.4 ±0.4	2.2 ±0.7
k_{FU}^{C}	3.8 ±0.4	5.9 ±0.2	1.3 ±0.2	1.4 ±0.4

The rates are given in Hz. The values are obtained averaging the results of 2 molecules for low trap stiffness and 5 and 7 molecules for high stiffness with short and long handles respectively. For each cell the top value is the average and the bottom value is the standard error.

S8. Effect of the stretching modulus on the effective rigidity of an elastic polymer

In this section we address the question of how the extensibility of a polymer modifies the rigidity associated to the entropic elasticity. Let us consider an inextensible polymer characterized by its entropic elasticity, $f_{L_0}(x) = \hat{f}\left(x/L_0\right)$ where x is the molecular extension and L_0 is the contour length. The corresponding rigidity of the inextensible polymer is given by $\varepsilon_i = (1/L_0) \times \left(\hat{f}\right)\left(x/L_0\right)$, meaning that, at a given force f, the rigidity of the handle ε_h is inversely proportional to the contour length. The extensibility of the polymer can be modeled by assuming that the contour length L_0 changes with force according to $L_0(1+f/Y)$ where f is the force and Y stands for the stretching modulus. It is straightforward to prove that the rigidity ε_e of the extensible polymer can be written as,

$$1/\varepsilon_e = 1/\varepsilon_i + x/Y\,, \tag{S12}$$

showing that only when $x >> Y/\varepsilon_i$ the contribution of the extensibility to the rigidity of the inextensible polymer is important. For dsDNA its elastic properties are well described by the worm-like chain model,

$$f = (k_B T/p) \times \left[\left(1/4(1-x/L_0)^2\right) - \left(1/4\right) + \left(x/L_0\right)\right], \tag{S13}$$

where p stands for the persistence length. Extensibility affects the rigidity of the polymer only when $x \cong L_0$ (i.e. when ε_i is maximum). In such limit we can approximate Eq. S13 by $f \approx \left(k_B T/4p\right)(1-x/L_0)^{-2}$ which gives

$$\varepsilon_i \approx k_B T/2pL_0\left[\left(4pf/k_B T\right)^{3/2} + 2\right] \approx \left(4f^{3/2}/L_0\right)\left(p/k_B T\right)^{1/2}, \tag{S14}$$

This expression can be introduced into Eq. S12 yielding,

$$1/\varepsilon_e \approx \left[\left(k_B T/p\right)^{1/2}\left(1/4f^{3/2}\right) + \left(1/Y\right)\right]L_0, \tag{S15}$$

For a linear dsDNA with $p \cong 50$nm and $Y \cong 1000$pN, the contribution of the extensibility property (i.e. the term $1/Y$ in Eq. S15) to the effective rigidity of the polymer starts to be important at forces above 10 pN. Equation S12 is a valid interpolation over a wide range of forces (above $\cong$1 pN). Note that for $f >>$ 20pN, ε_e is constant and given approximately by Y/L_0.

S9. Full table of results

Errors in this table are only statistical and do not include systematic instrumental uncertainties due to force and distance calibration errors (full errors combining statistical and instrumental uncertainties are given in Table 1 of main text and Table S5).

Table S9a. Kinetic and thermodynamic parameters for the 2S hairpin with short handles.

2S SH PM BELL - EVANS	f_{FU}^{C}	k_{FU}^{C}	$x_{FU}^{\ddagger}$	$x_{UF}^{\ddagger}$	x_{FU}	ΔG_{FU}
Mol1	14.71	1.47	9.79	8.79	18.58	66.48
Mol2	14.95	0.71	9.45	8.64	18.09	65.78
Mol4	15.19	0.96	9.63	7.84	17.47	64.56
Mol5	14.89	1.63	8.53	8.01	16.54	59.91
Mol6	14.45	1.73	9.15	8.15	17.30	60.81
Average	**14.8**	**1.30**	**9.31**	**8.28**	**17.59**	**63.5**
Statistical error	0.12	0.20	0.22	0.18	0.35	1.33

2S SH CFM BELL - EVANS	f_{FU}^{C}	k_{FU}^{C}	$x_{FU}^{\ddagger}$	$x_{UF}^{\ddagger}$	x_{FU}	ΔG_{FU}
Mol1	14.85	1.76	9.88	11.44	21.31	76.99
Mol4	15.19	0.97	9.79	9.33	19.12	70.64
Mol5	14.86	1.57	11.90	10.08	21.99	79.51
Mol6	14.46	1.66	9.80	9.47	19.27	67.78
Average	**14.8**	**1.49**	**10.3**	**10.1**	**20.42**	**73.7**
Statistical error	0.15	0.18	0.52	0.48	0.72	2.72

2S SH PM DETAILED BALANCE	f_{FU}^{C}	x_{FU}	ΔG_{FU}
Mol1	14.68	18.59	66.39
Mol2	14.92	18.16	65.91
Mol4	15.13	17.52	64.52
Mol5	14.87	16.55	59.88
Mol6	14.42	17.28	60.62
Average	**14.8**	**17.59**	**63.5**
Statistical error	0.12	0.35	1.35

2S SH CFM DETAILED BALANCE	f_{FU}^{C}	x_{FU}	ΔG_{FU}
Mol1	14.83	25.93	93.56
Mol4	15.15	18.26	67.27
Mol5	14.85	22.26	80.46
Mol6	14.45	18.87	66.34
Average	**14.8**	**21.3**	**76.9**
Statistical error	0.14	1.8	6.42

Table S9b. Kinetic and thermodynamic parameters for the 2S hairpin with long handles.

2S LH PM BELL – EVANS	f_{FU}^{C}	k_{FU}^{C}	$x_{FU}^{\ddagger}$	$x_{UF}^{\ddagger}$	x_{FU}	ΔG_{FU}
Mol1	15.43	5.32	9.94	7.44	17.38	64.85
Mol2	14.85	2.91	9.95	8.32	18.27	67.87
Mol3	14.63	4.09	9.7	9.54	19.24	68.49
Mol4	14.58	2.66	9.98	9.19	19.17	70.88
Mol5	14.68	3.57	10.27	8.58	18.85	67.33
Mol6	14.74	3.36	9.85	8.74	18.59	66.66
Average	**14.78**	**3.79**	**9.65**	**8.70**	**18.35**	**66.2**
Statistical error	0.12	0.36	0.30	0.26	0.33	1.20

2S LH CFM BELL – EVANS	f_{FU}^{C}	k_{FU}^{C}	$x_{FU}^{\ddagger}$	$x_{UF}^{\ddagger}$	x_{FU}	ΔG_{FU}
Mol2	14.86	3.6	11.96	10.41	22.37	80.48
Mol3	14.54	5.27	13.04	11.03	24.07	85.88
Mol4	14.67	3.06	12.13	10.03	22.16	79.53
Mol5	14.67	4.2	11.87	12.09	23.96	85.71
Mol6	14.73	3.83	11.83	11.08	22.91	82.67
Average	**14.69**	**3.99**	**12.17**	**10.93**	**23.09**	**82.85**
Statistical error	0.05	0.37	0.22	0.35	0.40	1.30

2S LH PM DETAILED BALANCE	f_{FU}^{C}	x_{FU}	ΔG_{FU}
Mol1	14.52	18.66	65.93
Mol2	14.81	17.71	63.79
Mol3	14.63	18.31	65.16
Mol4	14.56	18.85	66.77
Mol5	14.64	18.33	65.2
Mol6	14.72	18.03	64.55
Mol7	14.57	16.89	59.97
Average	**14.63**	**18.11**	**64.49**
Statistical error	0.04	0.25	0.83

2S LH CFM DETAILED BALANCE	f_{FU}^{C}	x_{FU}	ΔG_{FU}
Mol2	14.86	22.52	81.44
Mol3	14.54	24.11	85.31
Mol4	14.67	22.22	79.32
Mol5	14.69	22.75	81.30
Mol6	14.71	23.08	82.63
Average	**14.69**	**22.94**	**82.00**
Statistical error	0.051	0.32	0.98

Table S9c. Kinetic and thermodynamic parameters for the 3S hairpin with short handles.

3S SH PM ***Bell -Evans***	f_{FI}^{C}	f_{IU}^{C}	k_{FI}^{C}	k_{IU}^{C}	$x_{FI}^{\ddagger}$	$x_{IF}^{\ddagger}$	$x_{IU}^{\ddagger}$	$x_{UI}^{\ddagger}$
Mol1	14.60	12.88	6.59	9.18	7.78	7.33	6.16	3.26
Mol2	14.63	12.91	8.48	9.80	7.44	5.98	6.03	4.22
Mol3	14.60	12.88	6.66	9.29	7.83	7.25	6.11	3.36
Mol4	14.83	12.98	7.68	9.29	7.67	6.98	5.92	3.67
Mol5	14.82	12.91	5.54	7.37	6.19	6.40	6.40	5.90
Mol6	14.00	12.31	7.53	8.48	7.69	6.61	6.06	4.72
Mol7	14.73	12.69	4.50	8.49	7.36	6.38	5.01	5.49
Average	**14.6**	**12.8**	**6.71**	**8.84**	**7.42**	**6.71**	**5.95**	**4.4**
Statistical error	0.11	0.09	0.51	0.30	0.22	0.19	0.17	0.39
	x_{FI}	x_{IU}	x_{FU}	ΔG_{FI}	ΔG_{IU}			
Mol1	15.11	9.42	24.54	53.68	29.53			
Mol2	13.42	10.25	23.67	47.78	32.18			
Mol3	15.08	9.47	24.55	53.58	29.67			
Mol4	14.66	9.59	24.25	52.90	30.30			
Mol5	12.59	12.30	24.88	45.40	38.63			
Mol6	14.31	10.78	25.09	48.75	32.29			
Mol7	13.75	10.49	24.24	49.28	32.41			
Average	**14.1**	**10.3**	**24.5**	**50.2**	**32.1**			
Statistical error	0.35	0.38	0.18	1.22	1.18			

3S SH CFM ***Bell -Evans***	f_{FI}^{C}	f_{IU}^{C}	k_{FI}^{C}	k_{IU}^{C}	$x_{FI}^{\ddagger}$	$x_{IF}^{\ddagger}$	$x_{IU}^{\ddagger}$	$x_{UI}^{\ddagger}$
Mol1	14.49	13.31	5.93	5.34	5.00	10.46	11.22	3.70
Mol2	14.72	13.29	7.39	6.63	6.96	8.65	8.74	5.78
Mol3	14.04	12.97	4.33	6.28	7.80	12.90	11.18	2.38
Mol4	14.22	12.18	8.81	5.97	7.10	3.65	5.92	3.88
Mol5	13.75	13.08	3.92	18.02	5.26	17.53	9.68	9.30
Mol6	14.56	13.11	9.52	5.34	7.55	6.64	10.61	4.53
Mol7	14.55	13.00	6.86	5.54	5.43	7.78	7.86	4.34
Average	**14.33**	**12.99**	**6.68**	**7.59**	**6.44**	**9.66**	**9.32**	**4.85**
Statistical error	0.13	0.14	0.80	1.75	0.44	1.71	0.74	0.84
	x_{FI}	x_{IU}	x_{FU}	ΔG_{FI}	ΔG_{IU}			
Mol1	15.47	14.92	30.38	54.53	48.30			
Mol2	15.61	14.53	30.13	55.89	46.99			
Mol3	20.70	13.57	34.27	70.75	42.81			
Mol4	10.76	9.80	20.55	37.21	29.05			
Mol5	22.79	18.98	41.77	76.22	60.40			
Mol6	14.18	15.14	29.32	50.26	48.29			
Mol7	13.21	12.20	25.41	46.78	38.58			
Average	**16.10**	**14.16**	**30.26**	**55.95**	**44.92**			
Statistical error	1.60	1.07	2.52	5.12	3.66			

3S SH PM ***Detailed Balance***	f_{FI}^{C}	f_{IU}^{C}	x_{FI}	x_{IU}	x_{FU}	ΔG_{FI}	ΔG_{IU}
Mol1	14.55	12.79	15.54	8.95	24.50	55.03	27.85
Mol2	14.56	12.86	13.75	9.98	23.73	48.70	31.23
Mol3	14.55	12.79	15.47	9.02	24.49	54.77	28.07
Mol4	14.78	12.97	14.61	9.79	24.40	52.55	30.89
Mol5	14.65	13.67	16.50	10.40	26.90	58.82	34.59
Mol6	13.93	12.30	14.67	10.49	25.17	49.74	31.40
Mol7	14.65	12.74	14.21	10.19	24.41	50.65	31.61
Average	**14.5**	**12.9**	**15.0**	**9.83**	**24.8**	**52.9**	**30.8**
Statistical error	0.10	0.15	0.35	0.24	0.38	1.35	0.87

3S SH CFM ***Detailed Balance***	f_{FI}^{C}	f_{IU}^{C}	x_{FI}	x_{IU}	x_{FU}	ΔG_{FI}	ΔG_{IU}
Mol1	14.48	13.30	15.72	14.68	30.40	55.39	47.51
Mol2	14.73	13.29	15.56	14.60	30.15	55.76	47.20
Mol3	14.16	13.03	16.11	15.40	31.50	55.49	48.83
Mol4	14.20	12.17	10.91	9.72	20.63	37.70	28.78
Mol5	13.86	12.85	18.83	13.75	32.58	63.47	42.99
Mol6	14.57	13.09	14.25	14.87	29.12	50.54	47.34
Mol7	14.56	12.99	13.27	12.14	25.41	47.01	38.36
Average	**14.37**	**12.96**	**14.95**	**13.59**	**28.54**	**52.19**	**43.00**
Statistical error	0.12	0.14	0.94	0.76	1.57	3.09	2.74

Table S9d. Kinetic and thermodynamic parameters for the 3S hairpin with long handles.

3S LH PM ***Bell -Evans***	f_{FI}^{C}	f_{IU}^{C}	k_{FI}^{C}	k_{IU}^{C}	$x_{FI}^{\ddagger}$	$x_{IF}^{\ddagger}$	$x_{IU}^{\ddagger}$	$x_{UI}^{\ddagger}$
Mol1	14.35	12.27	15.32	12.49	8.22	5.39	4.99	4.59
Mol2	14.91	12.90	18.82	12.86	8.15	5.09	5.45	4.11
Mol3	14.90	12.78	21.82	11.39	8.70	3.81	6.20	3.75
Mol4	13.98	12.45	11.51	9.70	8.65	4.99	5.49	4.31
Mol5	14.37	12.38	22.92	12.45	7.61	4.52	5.88	3.49
Average	**14.50**	**12.56**	**18.08**	**11.78**	**8.27**	**4.76**	**5.60**	**4.05**
Statistical error	0.178	0.12	2.11	0.57	0.19	0.27	0.20	0.19

	x_{FI}	x_{IU}	x_{FU}	ΔG_{FI}	ΔG_{IU}
Mol1	13.62	9.58	23.21	47.56	28.62
Mol2	13.24	9.57	22.81	48.04	30.05
Mol3	12.51	9.96	22.48	45.38	30.97
Mol4	13.64	9.80	23.44	46.42	29.70
Mol5	12.14	9.37	21.51	42.46	28.22
Average	**13.03**	**9.66**	**22.69**	**45.97**	**29.51**
Statistical error	0.30	0.10	0.33	0.99	0.49

3S LH CFM ***Bell -Evans***	f_{FI}^{C}	f_{IU}^{C}	k_{FI}^{C}	k_{IU}^{C}	$x_{FI}^{\ddagger}$	$x_{IF}^{\ddagger}$	$x_{IU}^{\ddagger}$	$x_{UI}^{\ddagger}$
Mol1	14.97	13.32	16.13	10.98	9.29	4.94	6.11	7.45
Mol2	14.57	13.15	12.19	8.50	10.33	8.97	6.75	6.04
Mol3	14.57	12.85	9.54	8.70	6.22	6.31	6.70	7.49
Mol4	13.94	12.52	15.86	10.36	10.76	6.73	8.00	8.55
Mol5	14.11	12.74	19.36	7.69	9.79	5.27	9.48	6.66
Average	**14.43**	**12.92**	**14.62**	**9.25**	**9.28**	**6.44**	**7.41**	**7.24**
Statistical error	0.189	0.14	1.70	0.61	0.80	0.71	0.60	0.42

	x_{FI}	x_{IU}	x_{FU}	ΔG_{FI}	ΔG_{IU}
Mol1	14.23	13.57	27.81	51.86	44.00
Mol2	19.31	12.79	32.10	68.46	40.96
Mol3	12.53	14.20	26.73	44.44	44.42
Mol4	17.49	16.56	34.05	59.35	50.47
Mol5	15.07	16.14	31.21	51.75	50.07
Average	**15.72**	**14.65**	**30.38**	**55.17**	**45.98**
Statistical error	0.30	0.73	1.36	4.07	1.85

3S LH PM ***Detailed Balance***	f_{FI}^{C}	f_{IU}^{C}	x_{FI}	x_{IU}	x_{FU}	ΔG_{FI}	ΔG_{IU}
Mol1	14.23	12.28	13.87	9.33	23.21	47.96	27.93
Mol2	14.82	12.84	12.79	9.15	21.95	46.10	28.65
Mol3	14.85	12.64	11.21	9.21	20.43	40.50	28.41
Mol4	14.09	12.14	13.20	9.70	22.90	45.24	28.67
Mol5	14.20	12.26	13.00	8.64	21.64	44.88	25.82
Average	**14.44**	**12.43**	**12.82**	**9.21**	**22.03**	**44.94**	**27.90**
Statistical error	0.16	0.13	0.43	0.17	0.49	1.23	0.53

3S LH CFM ***Detailed Balance***	f_{FI}^{C}	f_{IU}^{C}	x_{FI}	x_{IU}	x_{FU}	ΔG_{FI}	ΔG_{IU}
Mol1	14.95	13.32	14.29	13.49	27.79	52.02	43.78
Mol2	14.60	13.15	18.10	12.46	30.57	64.34	39.89
Mol3	14.54	12.56	13.12	11.30	24.43	46.43	34.57
Mol4	13.92	12.52	17.66	16.31	33.98	59.86	49.73
Mol5	14.16	12.75	14.09	16.07	30.17	48.60	49.89
Average	**14.44**	**12.86**	**15.45**	**13.93**	**29.39**	**54.25**	**43.57**
Statistical error	0.17	0.16	1.01	0.98	1.58	3.40	2.93

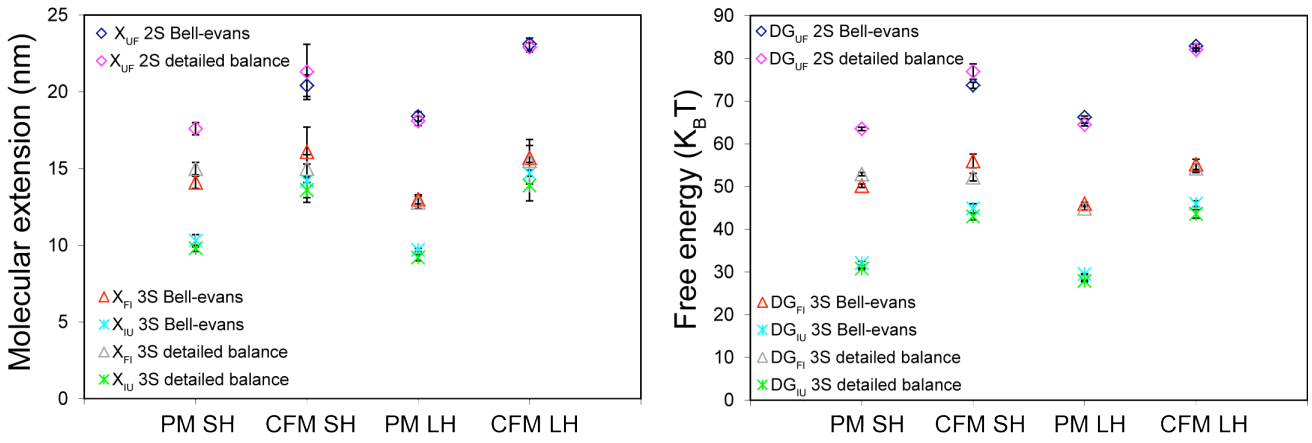

FIGURE S9: Results for the molecular distances (left panel) and free energies (right panel) as estimated from the Bell-Evans and detailed balance condition for the different experimental conditions tested (PM SH, CFM SH, PM LH, CFM LH). Results correspond to the average over 4-7 molecules (Table 1 main text).

REFERENCES

1. Liphardt, D., B. Onoa, S. B. Smith, I. Tinoco, Jr, and C. Bustamante. 2001. Reversible unfolding of single RNA molecules by mechanical force. *Science*. 292:733-737.

2. Fernández, J. M., S. Chu, and A. F. Oberhauser. 2001. Pulling on hair(pins). *Science*. 292:653-654.

3. Bonnet, G., O. Krichevsky, and A. Libchaber. 1998. Kinetics of conformational fluctuations in DNA hairpin-loops. *Proc. Nat. Acad. Sci. USA*. 95: 602-8606.

4. Li, P. T. X., D. Collin, S. B. Smith, C. Bustamante, and I. Tinoco, Jr. 2006. Probing the mechanical folding kinetics of TAR RNA by hopping, force-jump, and force-ramp methods. *Biophys. J*. 90:250-260.

5. Santalucia, J., Jr. 1998. A unified view of polymer, dumbbell, and oligonucleotide DNA nearest-neighbor thermodynamics. *Proc. Natl. Acad. Sci. USA*. 95:1460-1465.

6. Zuker, M. 2003. Mfold web server for nucleic acid folding and hybridization prediction. *Nucleic Acids Res*. 31:3406-3415.

7. Bustamante, C., and S. B. Smith. 2006. US Patent 7, 133, 132, B2(2006).

8. Huguet, J. M., N. Forns, and F. Ritort. 2009. Statistical properties of metastable intermediates in DNA Unzipping. *Phys. Rev. Lett*. 103:248106(4).

9. Mossa, A., M. Manosas, N. Forns, J. M. Huguet, and F. Ritort. 2009. Dynamic force spectroscopy of DNA hairpins: I. Force kinetics and free energy landscapes. *J. Stat. Mech*. 2009:P02060.

10. Wen J.-D., M. Manosas, P. T. X. Li, S. B. Smith, C. Bustamante, F. Ritort, and I. Tinoco, Jr. 2007. Force unfolding kinetics of RNA using optical tweezers. I. Effects of experimental variables on measured results. *Biophys. J*. 92:2996-3009.

11. Manosas, M., J.-D. Wen, P. T. X. Li, S. B. Smith, C. Bustamante, I. Tinoco, Jr., and F. Ritort. 2007. Force unfolding kinetics of RNA using optical tweezers. II. Modeling experiments. *Biophys. J*.92:3010-3021.

12. Greenleaf, W. J., M. T. Woodside, E. A. Abbondanzieri, and S. M. Block. 2005. Passive all-optical force clamp for high-resolution laser trapping. *Phys. Rev. Lett*. 95(20): 208102.

13. Liphardt, D., B. Onoa, S. B. Smith, I. Tinoco, Jr, and C. Bustamante. 2001. Reversible unfolding of single RNA molecules by mechanical force. *Science*. 292:733-737.

14. Onoa, B., D. Dumont, J. Liphardt, S. B. Smith, I. Tinoco, and C. Bustamante. 2003. Identifying kinetic barriers to mechanical unfolding of the *T. thermophila* ribozyme. *Science*. 299:1892-1895.